HHS Public Access

Author manuscript

Mater Sci Eng C Mater Biol Appl. Author manuscript; available in PMC 2020 March 09.

Published in final edited form as:

Mater Sci Eng C Mater Biol Appl. 2020 January ; 106: 110268. doi:10.1016/j.msec.2019.110268.

Electrospun Thymosin Beta-4 Loaded PLGA/PLA Nanofiber/ Microfiber Hybrid Yarns for Tendon Tissue Engineering Application

Shaohua Wu[1,2], **Rong Zhou**[2,3], **Fang Zhou**[2], **Philipp N. Streubel**[4], **Shaojuan Chen**[2,*], **Bin Duan**[1,5,6,*]

[1]Mary & Dick Holland Regenerative Medicine Program, and Division of Cardiology, Department of Internal Medicine, University of Nebraska Medical Center, Omaha, NE, USA

[2]College of Textiles & Clothing, Qingdao University, Qingdao, China

[3]Industrial Research Institute of Nonwoven & Technical Textiles, Qingdao University, Qingdao, China

[4]Department of Orthopedic Surgery and Rehabilitation, University of Nebraska Medical Center, Omaha, NE, USA

[5]Department of Surgery, College of Medicine, University of Nebraska Medical Center, Omaha, NE, USA

[6]Department of Mechanical and Materials Engineering, University of Nebraska-Lincoln, Lincoln, NE, USA

Abstract

Microfiber yarns (MY) have been widely employed to construct tendon tissue grafts. However, suboptimal ultrastructure and inappropriate environments for cell interactions limit their clinical application. Herein, we designed a modified electrospinning device to coat poly(lactic-co-glycolic acid) PLGA nanofibers onto polylactic acid (PLA) MY to generate PLGA/PLA hybrid yarns (HY), which had a well-aligned nanofibrous structure, resembling the ultrastructure of native tendon tissues and showed enhanced failure load compared to PLA MY. PLGA/PLA HY significantly improved the growth, proliferation, and tendon-specific gene expressions of human adipose derived mesenchymal stem cells (HADMSC) compared to PLA MY. Moreover, thymosin beta-4 (Tβ4) loaded PLGA/PLA HY presented a sustained drug release manner for 28 days and showed an additive effect on promoting HADMSC migration, proliferation, and tenogenic differentiation. Collectively, the combination of Tβ4 with the nano-topography of PLGA/PLA HY might be an efficient strategy to promote tenogenesis of adult stem cells for tendon tissue engineering.

*Corresponding authors: Dr. Shaojuan Chen, qdchshj@qdu.edu.cn; Phone: +86-138-5322-6032, Dr. Bin Duan, bin.duan@unmc.edu; Phone: +1-(402) 559-9637.

Appendix A. Supplementary data

The Supporting Information is available on the website.

Keywords

Nanofiber yarn; Core-sheath yarn; Drug delivery; Tenogenic differentiation; Cell migration

1. Introduction

Tendon is a bundle of fibrous connective tissue that plays a crucial role in our musculoskeletal mobility by providing stress transfer and joint stability [1]. However, tendon tissue is highly susceptible to be damaged by various physical exercises, tendon diseases and accidents, and it has an inherently poor healing capacity [2, 3]. Traditional clinical treatments for the augmentation and reconstruction of damaged tendon include autografts, allografts, and xenografts [4, 5]. These options have led to unreliable clinical outcomes, as these constructs provide a suboptimal mechanical and biochemical substrate to recreate the native tendon tissue [6, 7].

Tissue engineering (TE) has been recognized as a promising strategy for regenerative tendon repair [8, 9]. Many studies have emphasized the importance of appropriate design of fibrous scaffolds [10, 11], which could potentially mimic the fibrillary microarchitecture and the functional characteristics of native tendon extracellular matrix (ECM) [12–14]. At present, various fiber-fabricating techniques and textile processes have been employed to engineer and generate fibrous constructs [15, 16]. Two steps are commonly included, in which micrometer-scale yarns are produced through the wet or dry spinning process, and then are assembled into 2D or 3D constructs with tunable properties by textile technology, i.e., weaving, knitting, and braiding [17–19]. Recent studies have demonstrated that such textile-based scaffolds could uniquely combine precisely controlled size, shape, and excellent load-bearing and suture-retention strengths for tendon repair [20–22]. However, these textiles are generated from microfiber yarns (usually fiber diameter > 10 μm), which differ from the inherent nanoscale organization of collagen fibrils in native tendon ECM, inevitably resulting in reduced cellular activity and inferior regeneration outcome [23–25]. In the past few decades, electrospinning techniques have been developed to manufacture scaffolds with smaller diameter fibers [26–28]. The diameter of the fibers produced using electrospinning is in the range of 50–1000 nm, which is two to three orders of magnitude smaller than that formed by traditional fiber-fabrication processes [29, 30]. Electrospun nanofibrous scaffolds can closely mimic the diameter scale and topographical cues of collagen fibrils of native tendon ECM [31, 32], and have been extensively studied for tendon repair, showing excellent *in vitro* performance in terms of cell adhesion, spreading, and tenogenic differentiation of stem cells [33, 34]. However, most of these electrospun scaffolds are too weak to be surgically implanted or to mechanically support the primary tendon healing, especially for large animals and human [35–37]. Therefore, better scaffold design and fabrication recreating both tendon ECM-like hierarchical ultra-structures and bio-mechanical properties is urgently needed.

Another important aspect for tendon TE is how to promote tenogenic differentiation of stem cells and scar-less tendon healing [38–40]. Mesenchymal stem cells (MSC) have come to the forefront of tendon TE, due to their availability and tenogenic differentiation capacity [41,

42]. Previous studies demonstrated that the outcomes with fibrous scaffolds alone are unsatisfactory for tendon regeneration in animal models [43, 44]. Bioactive factor stimulation is recognized as a potential method to promote MSC tenogenesis in previous literatures [45–47]. This requires drugs and/or growth factors to be incorporated into fibrous scaffolds to regulate the differentiation of MSC. Thymosin beta-4 (Tβ4), a highly conserved water-soluble peptide factor, is found to be naturally produced in higher concentration in locations of tendon damage, promoting multiple biological activities including the promotion of scar-less tissue healing [48–50]. Tβ4 has also been demonstrated as a potent anti-inflammatory agent [51, 52]. Moreover, recent studies have shown that Tβ4 treatment could result in stem cell activation, direct cell migration and mediation of cell differentiation. The positive healing effect of Tβ4 has been observed in tendon, ligament, skin, heart and brain tissue [53–55].

To optimize TE matrices, we aimed to modify the commercially textile-used and biodegradable polylactic acid (PLA) microfiber yarns (MY) and generate a mechanically-strong, nano-surface-possessed and bioactive-factor-involved hybrid yarns (HY) for tendon TE application. We first implemented a novel electrospinning device to continuously coat the PLA MY with poly(lactic-co-glycolic acid) (PLGA) nanofibers, thereby obtaining PLGA/PLA nanofiber/microfiber hybrid yarns (HY). PLA microfibers thereby provide mechanical and structural resistance, while the coated PLGA nanofibers are expected to improve the biological properties. In this study, we compared the structural and mechanical properties of PLA MY and PLGA/PLA HY. Furthermore, we compared human adipose derived mesenchymal stem cells (HADMSC) response to these two different yarns. Finally, we employed our PLGA/PLA HY as a drug delivery vehicle to encapsulate Tβ4, and investigated how the release of Tβ4 affected cell behaviors, including cell proliferation, migration, and tenogenic expression of HADMSC.

2. Materials and methods

2.1 Fabrication of PLGA/PLA HY with or without incorporation of Tβ4

A novel electrospinning setup was designed and implemented by our group as shown in Fig. 1A. We employed a yarn-supply roll and one set of tension device to continuously convey PLA MY (Shaoxing Zhongfangyuan Co., Ltd, China). The PLA filament diameter was about 15 μm and the filament number was 18 for each PLA multifilament yarn. Two oppositely placed metal needles were applied with positive and negative voltages to generate PLGA (82/18 LG/GA, Corbion Purac) nanofibers. Two solution supplies were utilized to supply polymer solutions for the two metal needles with controllable solution flow rates. A rotating neutral metal disc (NMD) and a static neutral hollow metal rod (NHMR) placed oppositely in the middle of two needles were employed to collect and coat PLGA nanofibers on PLA MY and further process them into PLGA/PLA HY. The obtained PLGA/PLA HY were passed through the inner part of NHMR and gathered on a rotating collecting roll. For the fabrication of pure PLGA/PLA HY (without Tβ4), PLGA (1.2 g) was first dissolved in 8 mL of hexafluoro-2-propanol (HFIP, Acros Organics) under stirring to obtain a homogeneous solution. Then PLGA solution was electrospun to generate PLGA/PLA N/M HY using our electrospinning setup with the following processing parameters: distance

between two needles 20 cm, distance between NMD and NHMR 7 cm, applied voltages of two needles ±12 kV, solution flow rate of both needles 1 mL/h, rotation speed of NMD 250 r/min, and linear velocity of take-up roll 2 m/min. For the fabrication of Tβ4-loaded PLGA/PLA HY, two different dosages of Tβ4 (0.04 mg, or 0.4 mg) were dissolved in 500 μL 1 % bovine serum albumin (BSA) solution and then mixed with PLGA (1.2 g), Span 80 (100μL) and HFIP (8 mL) solution to form Tβ4/PLGA emulsion under stirring. Tβ4/PLGA emulsion was further electrospun to generate Tβ4-loaded PLGA/PLA HY using the same processing parameters as described for PLGA/PLA HY fabrication. Based on Tβ4 content, two different Tβ4 loaded PLGA/PLA HY were fabricated and denoted as L-Tβ4 PLGA/PLA HY (with low Tβ4 dosage: 0.04 mg Tβ4 in 1.2 g PLGA) and H-Tβ4 PLGA/PLA HY (with high Tβ4 dosage: 0.4 mg Tβ4 in 1.2 g PLGA), respectively.

2.2 Morphological and mechanical characterization of the yarn materials

Samples were examined via a scanning electron microscope (SEM, FEI Quanta 200) for morphology assessment after gold coating. The fiber diameter, yarn diameter and fiber angle distribution (relative to the horizontal axis) of the specimens (n = 3) were determined from the SEM images using Image J software (National Institutes of Health, USA). The angle distribution and mean diameter were determined from more than 100 randomly selected nanofibers in the SEM images. Uniaxial tension tests were performed using a XQ-2 fiber strength tester (Shanghai Lipu Institute of Applied Science and Technology, Shanghai, China). The tests were performed with a gauge length of 10 mm at a constant rate of 10 mm/min until failure occurred. Twenty specimens were tested for each sample. The Young's modulus at 5%−10% strain, ultimate stress and strain were determined.

2.3 Tβ4 release behavior from the hybrid yarns

Tβ4 loaded PLGA/PLA HY were immersed in individual centrifuge tubes containing 2 mL of phosphate buffer saline (PBS, pH 7.4) solutions, and all the tubes were kept in a shaking water bath at 37 °C. The PBS solutions were replaced with fresh PBS solutions at predetermined time intervals throughout 28 days. The Tβ4 concentration was measured using human Tβ4 ELISA Kit Assay (RayBiotech). The drug-release studies were performed in triplicate for all the conditions.

2.4 Cell seeding, culture and differentiation

Primary HADMSC were purchased from Lonza and cultured in growth medium (GM) consisting of DMEM/F12 (Invitrogen), 10 % FBS (Invitrogen) and 1% P/S (Invitrogen). HADMSC were used at passages 4–6. Tendon medium (TM) with DMEM/F12 medium, 2% FBS, 20 ng/ml TGFβ3 (PeproTech), was employed to induce tenogenic differentiation of HADMSC [23, 34]. In order to investigate the effects of Tβ4 on HADMSC in 2D culture, HADMSC were seeded in a 6-well plate at the density of 5000 cells per well with addition of Tβ4 (0, 40, 400, or 4000 ng Tβ4 in 4 mL TM per well). For cell seeding and culture on all the yarn samples, yarns were trimmed into the length of 2.2 cm, and were bundled together (15 yarns) using 5% (w/v) sodium alginate solution and 5% (w/v) calcium chloride solution as glue. Before cell seeding, the samples were sterilized by UV light for 2 h. The yarn bundles were transferred into silicone molds (22 mm length × 3 mm width, 1 mm thickness) for cell seeding. The HADMSC were seeded at a density of 1×10^5 cells per yarn bundle. For

all the cell culture experiments, cells were cultured in 5 % CO_2 at 37 °C, and the medium was replaced every 2 days.

2.5 Cell Viability, proliferation and migration characterization

The viability and morphology of HADMSC cultured in different conditions were characterized by Live/Dead assay (Invitrogen) as previously described [24]. Calcein AM was utilized to stain the live cells, producing an intense green fluorescence in live cells. EthD-1 entered cells with damaged membranes and binded to nucleic acids, thereby producing a red fluorescence in dead cells. After 30 min incubation and staining, a confocal laser scanning microscopy (CLSM, LSM 710, Carl Zeiss) was employed to obtain fluorescence images. The cell proliferation tests of HADMSC on different scaffolds were conducted at predetermined time intervals by using MTT assay [34]. Cell-seeded yarn bundles were transferred into a 24 well plate. 1 ml fresh cell culture medium and 100μl MTT solution (5mg/ml) were further added. After 4 h incubation, the solution was removed, and DMSO (500 μl/well) were added to dissolve the formed formazan crystals. After all the formazan crystals were dissolved, 100μl formazan-DMSO solution was transferred to a 96 well plate. The absorbance value at the wavelength of 540 nm were measured by using a microplate reader (Bio-Tek Instruments). The cell migration behavior on different yarn samples were examined by using a 3D printed rectangular frame with the sizes of 3 cm ×1.5 cm, as shown in Fig. 5B. The yarns were twined to the frame as a bundle (with 15 yarns). HADMSC were seeded on one end of yarn bundle at a density of 1×10^5 cells, and the cell migration and proliferation behaviors were continuously observed throughout 21 days by using MTT assay.

2.6 Immunofluorescent (IF) staining

For IF staining, HADMSC-seeded samples were fixed in 4% paraformaldehyde, permeabilized in 0.2% Trion X-100 and then blocked with 1% BSA overnight at 4 °C [23]. The cell-seeded samples were then treated with primary antibodies to tenomodulin (TNMD, 1:50, Abcam), collagen type I (COL1, 1:100, Santa Cruz Biotechnology) overnight at 4 °C. Secondary fluorescent antibodies were incubated for 2 h and nuclear counterstaining (Draq 5, 1: 1000, Thermo Scientific) were performed for 30 minutes at room temperature. The stained samples were imaged with Zeiss 710 CLSM.

2.7 Total collagen content test

On day 21, the constructs were washed in PBS and dried using a vacuum freeze-drier (LABCONCO). After dry weight measurement, total collagen content was determined using a hydroxyproline assay [56]. The collagen values were calculated assuming 12.5% of collagen is hydroxyproline.

2.8 RNA isolation and qPCR

QIA-Shredder and RNeasy mini-kits (QIAgen) were utilized to extract total from cell-seeded constructs, according to the manufactures' instructions [23]. Total RNA was synthesized into first strand cDNA in a 20 μL reaction using iScript cDNA synthesis kit (BioRad Laboratories, USA). Real-time PCR analysis was performed in a StepOnePlus™

Real-Time PCR System (Thermo Scientific) using SsoAdvanced SYBR Green Supermix (Bio-Rad). cDNA samples were analyzed for the gene of interest and for the housekeeping gene 18S rRNA. The level of expression of each target gene was calculated using comparative Ct ($2^{-\Delta\Delta Ct}$) method. All primers used in this study are listed in Supplementary Table S1.

2.9 Statistical Analysis

All quantitative data were expressed as mean ± standard deviation (SD). Pairwise comparisons between groups were conducted using ANOVA with Scheffé post-hoc tests in statistical analysis. A value of $p<0.05$ was considered statistically significant.

3. Results

3.1 Morphology and mechanical properties of electrospun PLGA/PLA HY

A schematic illustration presents the hybrid yarn fabrication process by using our modified electrospinning device (Fig. 1A). During the coating of electrospun PLGA nanofibers, two charged jets of PLGA solution erupted from the oppositely charged nozzles were attracted and collected between NMD and NHMR hence neutralizing the oppositely charged jets. By fastening the NHMR and rotating the NMD, twisted PLGA nanofibers were coated on the surface of PLA MY. Twisting could cause more interaction and greater cohesion between PLGA nanofibers and PLA MY in the resultant PLGA/PLA HY structure. In the current study, we tended to obtain the more aligned PLGA nanofibrous structure to mimic the aligned fibril structure in the native tendon, so a relatively low twist (about 1.25 twists of 10 mm) was employed. A package of PLGA/PLA HY demonstrated that HY production with this system was reproducible in a continuous and large-scale manner (Fig. 1B). With this system, we can easily produce PLGA/PLA HY with near limitless length at the productivity rate of roughly 10 meters/min. SEM images (Fig. 1C and D) show the original uncoated PLA MY. The average diameters for PLA MY and individual fiber were 163.5±14.6 μm, and 16.2±0.6 μm, respectively. SEM images of the fabricated PLGA/PLA HY are shown in Fig. 1E and F. Generally, PLA MY were evenly and completely covered by a thin layer of PLGA nanofibers, without exposure of PLA MY on the HY surface. The average diameter of the PLGA/PLA HY slightly increased to 172.8±6.4 μm after the electrospinning coating process. Moreover, the PLGA nanofibers presented a highly smooth morphology without the occurrence of bead defects on the surface (Fig. 1F). The PLGA nanofibers had a relatively uniform diameter distribution with the mean value of 663.5±200.8 nm (Fig. 1G). It was also found that more than 90% of PLGA nanofibers were highly aligned along the HY longitudinal direction (within ±30°, Fig. 1H).

Mechanical performance is one of the essential requirements for structure-supportive tendon scaffold, as tendons are subjected to dynamic mechanical forces *in vivo*. Fig. 2A–E show the representative load-elongation curves and calculated mechanical properties of both PLA MY and PLGA/PLA HY. The results showed that PLGA/PLA HY had a higher failure load than the PLA MY (277.7 ± 9.0 cN for HY vs. 253.6 ± 10.7 cN for MY, $p<0.01$, Fig. 2B). There was no significant difference for ultimate tensile strength (Fig. 2C), Young's moduli (Fig. 2D) and strain at failure (Fig. 2E) between PLA MY and PLGA/PLA HY. The mechanical

property results indicate that the inner PLA microfibers are the primary providers of structural integrity and mechanical properties for the obtained PLGA/PLA HY. The coated PLGA nanofibers may slightly improve the load resistance capacity of PLGA/PLA HY, which was possibly attributed to an increase of internal forces produced between nanofibers and microfibers.

3.2 PLGA/PLA HY promoted HADMSC proliferation, alignment and tenogenic differentiation

We first seeded HADMSC on PLA MY bundles and PLGA/PLA HY bundles, then cultured them in TM for 21 days to determine how the matrix structure and topography affect cell behaviors. HADMSC cultured on the two yarn bundles showed high viability with very few dead cells (Fig. 3A, B). However, cell morphology varied in response to different yarn topography. HADMSC on the PLA MY bundles exhibited a less-expanded and irregular-patterned morphology (Fig. 3A). In contrast, cells on PLGA/PLA HY were well attached and showed a spindle-shaped morphology, with extensive alignment along the nanofibers (Fig. 3B and Fig. S1). These indicated that HADMSC could sense the nanofiber-based topographic features and regulate their morphology by contact guidance phenomenon. A MTT assay was utilized to evaluate the proliferation of HADMSC on the two yarn bundles. The results demonstrated that the cell proliferation rate on the PLGA/PLA HY bundles was significantly higher than that on the PLA MY bundles at days 1, 7, and 21 (Fig. 3C).

Tendon-related protein markers were detected by IF staining (Fig. 3D–G). Higher expressions of TNMD and COL1 were observed in HADMSC cultured on PLGA/PLA HY bundles than those on PLA MY bundles. Importantly, the surface modification by coating with PLGA nanofibers also guided robust protein secretion along the nanofiber alignment, which could better mimic the ECM architecture of native tendon tissues (Fig. S2). In order to further evaluate phenotypic change of HADMSC, tenocyte-specific gene expressions were quantified by qPCR (Fig. 3H). Scleraxis (SCX) is a necessary transcription factor for tenogenesis, and tenascin C (TNC) is an early marker in embryonic tendon. COL1 and COL3 are the primary matrix components of native tendons, and TNMD is recognized as late marker for the mature tenogenic phenotype. We found that HADMSC on PLGA/PLA HY group had significantly upregulated SCX (6.6±2.4-fold increase; $p<0.05$), TNC (8.0±2.8-fold increase; $p<0.05$), COL1 (2.9±0.3-fold increase; $p<0.01$), and TNMD (4.1±1.5-fold increase; $p<0.05$) gene expression compared to those on PLA MY group. These results confirmed that the PLGA/PLA HY promoted tenolineage differentiation of HADMSC better than PLA MY. Together, these results demonstrated that the nanofibrous surface on the PLGA/PLA HY was notably effective in enhancing cell attachment, growth, proliferation, and tenogenic differentiation.

3.3 Tβ4 treatment increased HADMSC proliferation and upregulated the expression of tendon-specific markers in 2D culture

We first evaluated the dose- and time-dependent effects of Tβ4 on the proliferation rate of HADMSC in 2D culture. HADMSC cultured in 2D plate were treated with different concentrations of Tβ4 (0, 10, 100, and 1000 ng/mL) for 14 days. Live/dead assay showed that HADMSC cultured in all four groups possessed high cell viability (Fig. 4A). The MTT

results demonstrated that the number of cells cultured in all groups continued to increase up to day 14 (Fig. 4B). At day 1, the MTT absorbance for the three groups with Tβ4 treatment was significantly higher than the control group (without Tβ4). In addition, a statistical difference was also found between the 10 and 1000 ng/mL Tβ4 treated groups. At day 7, HADMSC proliferation rate also increased with the increasing Tβ4 dose, but there was no statistical difference between the 100 and 1000 ng/mL Tβ4 treated groups. At day 14, the cell number was observed to be significantly increased in the group treated with 1000 ng/mL of Tβ4 in comparison with control group.

IF staining and qPCR tests were further employed to evaluate the effects of Tβ4 on tenogenic differentiation of HADMSC. The expression of TNMD and COL1 was detected in all four groups, and increased in a Tβ4 concentration-dependent manner (Fig. 4C, D). As shown in Fig. 4E, HADMSC showed higher gene expressions of SCX, TNC, COL1, and TNMD in all the three Tβ4 treated groups than those in the control group. In addition, the expressions of these four genes presented an increasing trend with the increase of the Tβ4 concentration. There was no statistical difference for SCX, COL1 and TNMD gene expressions between the 100 and 1000 ng/mL Tβ4 treated groups, and for TNC gene expression between the 10 and 100 ng/mL Tβ4 treated groups. The COL3 gene expression was comparable in both control and 10 ng/mL Tβ4 treated groups, and largely increased in the groups with high dosages of Tβ4. Taken together, these results demonstrated that the treatment of Tβ4 promoted proliferation and tenogenic differentiation of HADMSC in 2D culture.

3.4 Incorporation of Tβ4 into PLGA/PLA HY presented an additive effect on promoting HADMSC migration, proliferation, collagen secretion and tenogenic differentiation

The cumulative release profiles of Tβ4 from the L-Tβ4 PLGA/PLA HY and H-Tβ4 PLGA/PLA HY were shown in Fig. 5A. Tβ4 release kinetics from both of PLGA/PLA HY were similar and characterized with a typical biphasic stage: an initial burst release followed by a steadier and slower release. The drug release amount from the L-Tβ4 PLGA/PLA HY and H-Tβ4 PLGA/PLA HY were 10.3±2.2 and 129.4±4.6 ng/mg nanofibers for the first 3 days, and reached to 18.5±1.8 and 190.7±16.4 ng/mg nanofibers for the whole 28 days. The initial burst release was limited in our systems, indicative of relatively homogenous dispersion of encapsulated Tβ4 molecules within the PLGA/PLA HY.

The migration and proliferation of HADMSC on the surface of PLA MY and PLGA/PLA HY (with or without Tβ4) bundles was compared on our 3D printed frames after 1, 7, and 21-day cultures (Fig. 5B). At day 1, the cells attached and concentrated on one end of the yarn bundles in the four groups, and no significant difference on cell migration was observed between these four groups. At day 7 and 21, HADMSC on the PLGA/PLA HY (without Tβ4) bundles exhibited an obviously higher cell migration rate than those on PLA MY bundles, confirming that the nanofibers on the PLGA/PLA HY could provide a favorable surface for cell attachment and migration. The encapsulation and release of Tβ4 in PLGA/PLA HY further enhanced the migration of HADMSC. The MTT results demonstrated that the combination of PLGA nanofibrous surface and Tβ4 had an additive effect on increasing the proliferation rate of HADMSC (Fig. 5C). The differentiated

HADMSC also showed high cell viability and extensively expressed TNMD on the PLGA/PLA HY with both low and high dose of Tβ4 (Fig. S3).

Collagen is the primary component ECM in native tendon, which plays an important role in maintaining the inherent structure and regulating the biological function of tendon tissue. Therefore, the total collagen content was detected on the four different HADMSC-seeded yarn bundles after 21day culture (Fig. 5D). The results showed that the lowest collagen content was observed in PLA MY group, and the collagen content presented a notably increasing trend on PLGA/PLA HY bundles with increasing Tβ4 dosage. We finally compared the tenogenic lineage-related gene expression level of HADMSC cultured on the PLGA/PLA HY bundles (with or without Tβ4) on day 21 (Fig. 5E). The results showed that the expressions of SCX, TNC, COL1, COL3, TNMD of HADMSC on the two groups with Tβ4 were significantly upregulated compared with PLGA/PLA HY alone group. Together, these results demonstrated that the effective combination of bioactive factor (Tβ4) with aligned nanofibrous surface topography (PLGA nanofibers) provided an instructive microenvironment for HADSMC activities, from the migration and proliferation, to collagen secretion and tenogenic differentiation.

Discussion

Native tendon tissue possesses the hierarchical architecture at various scale-levels, consisting of intensively packed aligned collagen fibrils (50–500 nm in diameter), which in turn organize to collagen fibers, and further form a higher level of collagen fascicles (150–1000 μm in diameter) [57, 58], as shown in Fig. S2. In the design of a biomimetic scaffold for tendon regeneration, it is important to consider the high complexity of the natural tendon fibrous structure. Recently, the advances in engineering and knowledge of chemistry and biology have brought several fiber-fabrication technologies, which enable to mimic the tendon fibrous structure ranging from the nanometer to millimeter scale [37, 59]. For instance, the traditional textile techniques, like wet spinning or dry spinning, are commonly selected to mimic the collagen fibers with a diameter of less than 100 μm [60, 61]. Electrospinning has been recognized as a simple and straightforward method for nanofiber fabrication, which replicates the collagen fibrils [62, 63]. In our current study, we modified the typical electrospinning setup and developed a novel setup for continuously coating nanofibers onto biodegradable PLA microfiber yarns. By using this method, we successfully generated PLGA/PLA HY, which could combine the advantages of both nanofibers and microfibers to better resemble the tendon fibrous structure. Moreover, multiple PLGA/PLA HY were employed to form bundles for the replication of the hierarchical architecture of tendon fibers.

Engineering the topography of biomaterial scaffolds is an effective way to control the cell fate by mimicking the natural contact-mediated signaling events. Cells can sense and reshape in response to surface pattern features [64]. In this study, a uniform PLGA nanofibrous surface with a well-aligned fiber orientation was created on the PLA MY. The present results demonstrated that coating of electrospun PLGA nanofibers on PLA MY provided more cell adhesion sites, and significantly improved the proliferation, tendon-like ECM deposition, and tenogenic differentiation of HADMSC, compared to PLA MY. As

supported by prior studies, our findings confirmed that the combination of reduced fiber scale and aligned topography, guided cell alignment and organization, promoted the cell proliferation and differentiation, and introduced the collagen fibril formation along the arrangement direction of fibers, which resembled the collagen fibril order and structure of native tendon ECM [12, 65].

Apart from its hierarchical architecture, tendon is a connective tissue experiencing dynamic mechanical forces *in vivo*, which makes mechanical strength one of its the key properties [66, 67]. Strength is required to maintain the integrity and mechanical properties of tendon scaffolds during implantation and support loads until sufficient host tissue regeneration has occurred [68, 69]. Some synthetic materials including PLA, polyglycolic acid (PGA), and their copolymer PLGA are the most popular polymers in tendon TE, due to their biodegradability and biocompatibility [70–73]. Previous studies have indicated that PGA is mechanically stronger than PLA. However, PGA degrades at a faster rate, with mechanical strength decreasing rapidly after 2 to 4 weeks after implantation [74]. PLA MY may provide a more beneficial scaffolding material than PGA MY, as they maintain their mechanical properties for more than 12 months in tendon TE [41, 75, 76]. We therefore selected PLA MY as the base yarns to fabricate PLGA/PLA HY in our current study. Other studies indicated that the hydrophobicity of PLA could leaded to relatively low cell response in comparison with PLGA [77], and we thus coated electrospun PLGA nanofibers on the surface of PLA MY. The results showed that the hybrid structure of PLGA/PLA HY maintained mechanical integrity from the microfibers and provided a favorable surface for cell interaction from the nanofibers. Importantly, by changing the number of PLA MY in the hybrid structure and selecting the appropriate textile technique, including bundling, braiding, weaving and knitting, the mechanical properties of the final structure can be adapted to different natural tendon tissues properties.

Previous studies have indicated that fibrous scaffolds alone do not yield satisfactory outcomes of tendon repair [78, 79]. Therefore, incorporating bioactive molecules with ultra-structures is critical in controlling stem cell fate in terms of cellular spatial arrangement and directional migration as well as cell proliferation and differentiation towards tenocytes in tendon TE. However, how to effectively introduce and accelerate MSC differentiation and maturation towards tenocytes still remains a challenging [80–82]. In the present study, we incorporated bioactive protein Tβ4 into electrospun PLGA nanofibers to provide effective biochemical clues for the hybrid yarns. The Tβ4 loaded PLGA nanofibers exhibited acceptable burst release of Tβ4 during the early stage and long-term sustained release of Tβ4 for about 28 days. Our preliminary experiment has demonstrated the function of Tβ4 in enhancing the proliferation and tenogenic differentiation of HADMSC in 2D culture. Furthermore, compared to PLGA/PLA HY alone, Tβ4 incorporated PLGA/PLA HY could not only orientate the alignment of HADMSC but also promote cell proliferation at a higher rate. As expected, Tβ4 incorporated HY also more effectively promoted teno-differentiation of HADMSC than HY alone as evidenced by tendon-specific proteins and genes expression. Interestingly, it was found that the encapsulation of Tβ4 into HY could significantly promote HADMSC migration compared with the HY alone. This plays a key role in to achieve early bridging of damaged tendon tissues *in vivo*. Other studies have demonstrated Tβ4 to promote cell migration, and enhance tendon repair and scarless wound healing [48, 50, 83].

Our data confirmed that the integration of topographical and chemical cues promoted better tenogenic commitment of HADMSC compared with an individual physical stimulation.

In summary, our Tβ4 loaded PLGA/PLA HY has four major advantages for tendon TE: (1) imitation of the hierarchically and anisotropically aligned structure of tendon ECM in various scales ranging from nanometer to micrometer level, (2) robust tendon mechanical properties, (3) recreation of essential topographical and biochemical features for migration, proliferation, alignment and tenogenic differentiation of HADMSC, and (4) potential for development of further complex architectures by textile-forming technology. Clinically, it is envisioned that our Tβ4 loaded PLGA/PLA HY could be effectively utilized to create regenerating tendon tissue constructs for connective tissue engineering. Future studies should further elucidate the signaling pathway of the interplay of nanofibrous topography and biochemical cues during tenogenic differentiation using Tβ4 loaded PLGA/PLA HY. Furthermore, the *in vivo* validation of these tissue-engineered tendon constructs will be required.

Conclusions

In this study, we developed a novel approach and electropinning setup for nano-surface coating of biodegradable PLA microfiber yarns with conformal layers of electrospun PLGA nanofibers. A bioactive protein factor, Tβ4, was further encapsulated into PLGA nanofibers during electrospinning process, resulting in nano-surface-possessed and bioactive-factor-involved PLGA/PLA HY for tendon TE application. The additive effects of PLGA nanofibers coating and Tβ4 incorporating endowed the modified PLGA/PLA HY with both contact-guidance and bioactive chemical cues, which provided an instructive microenvironment for HADMSC behaviors in terms of cell proliferation, directional alignment and migration, collagen secretion, and tenogenic differentiation. Meanwhile, the inherent PLA microfibers in the PLGA/PLA HY supplied robust mechanical performances for the structural integrity and load resistance. The Tβ4 loaded PLGA/PLA HY demonstrated great similarity with native tendons in architectural features, mechanical properties, and facilitate biological functionality. This study therefore provides key insights into the regulation of the tenogenic differentiation of stem cells and the fabrication of native ECM-like biological substitutes for tendon regeneration.

Supplementary Material

Refer to Web version on PubMed Central for supplementary material.

Acknowledgements

This work has been supported by Mary & Dick Holland Regenerative Medicine Program start-up grant, Nebraska Research Initiative funding, and National Institutes of Health (R01 AR073225) to B.D.. S.C. thanks for the support from Chinese science and technology major projects (2017YFB0309805-02 and 2018GGX108003). Support for the UNMC Advanced Microscopy Core Facility was provided by the Nebraska Research Initiative, the Fred and Pamela Buffett Cancer Center Support Grant (P30CA036727), and an Institutional Development Award (IDeA) from the NIGMS of the NIH (P30GM106397). The authors declare no competing financial interest.

References

[1]. Lomas A, Ryan C, Sorushanova A, Shologu N, Sideri A, Tsioli V, Fthenakis G, Tzora A, Skoufos I, Quinlan LR, Advanced drug delivery reviews, 84 (2015) 257–277. [PubMed: 25499820]

[2]. Longo UG, Lamberti A, Maffulli N, Denaro V, British medical bulletin, 98 (2010) 31–59. [PubMed: 20851817]

[3]. Tan S, Selvaratnam L, Ahmad T, JUMMEC: Journal of Health and Translational Medicine (Formerly known as Journal of the University of Malaya Medical Centre), 18 (2015) 12–25.

[4]. Zeugolis D, Chan J, Pandit A, Tendons: engineering of functional tissues, Tissue engineering, Springer, 2011, pp. 537–572.

[5]. Longo UG, Lamberti A, Maffulli N, Denaro V, British medical bulletin, 94 (2010) 165–188. [PubMed: 20047971]

[6]. Deng D, Wang W, Wang B, Zhang P, Zhou G, Zhang WJ, Cao Y, Liu W, Biomaterials, 35 (2014) 8801–8809. [PubMed: 25069604]

[7]. Tellado SF, Balmayor ER, Van Griensven M, Advanced drug delivery reviews, 94 (2015) 126–140. [PubMed: 25777059]

[8]. Walden G, Liao X, Donell S, Raxworthy MJ, Riley GP, Saeed A, Tissue Engineering Part B: Reviews, 23 (2017) 44–58. [PubMed: 27596929]

[9]. Dhandayuthapani B, Yoshida Y, Maekawa T, Kumar DS, International journal of polymer science, 2011 (2011).

[10]. Zhang X, Bogdanowicz D, Erisken C, Lee NM, Lu HH, Journal of shoulder and elbow surgery, 21 (2012) 266–277. [PubMed: 22244070]

[11]. Zhang C, Yuan H, Liu H, Chen X, Lu P, Zhu T, Yang L, Yin Z, Heng BC, Zhang Y, Biomaterials, 53 (2015) 716–730. [PubMed: 25890767]

[12]. Yin Z, Chen X, Chen JL, Shen WL, Nguyen TMH, Gao L, Ouyang HW, Biomaterials, 31 (2010) 2163–2175. [PubMed: 19995669]

[13]. Deepthi S, Sundaram MN, Kadavan JD, Jayakumar R, Carbohydrate polymers, 153 (2016) 492–500. [PubMed: 27561521]

[14]. Thayer PS, Verbridge SS, Dahlgren LA, Kakar S, Guelcher SA, Goldstein AS, Journal of Biomedical Materials Research Part A, 104 (2016) 1894–1901. [PubMed: 27037972]

[15]. Tamayol A, Akbari M, Annabi N, Paul A, Khademhosseini A, Juncker D, Biotechnology advances, 31 (2013) 669–687. [PubMed: 23195284]

[16]. McCullen SD, Haslauer CM, Loboa EG, Journal of Materials Chemistry, 20 (2010) 8776–8788.

[17]. Ribeiro VP, Silva-Correia J, Nascimento AI, da Silva Morais A, Marques AP, Ribeiro AS, Silva CJ, Bonifácio G, Sousa RA, Oliveira JM, Biomaterials, 123 (2017) 92–106. [PubMed: 28161684]

[18]. Huang X, Huang G, Ji Y, guang Ao R, Yu B, long Zhu Y, The Journal of Foot and Ankle Surgery, 54 (2015) 1004–1009. [PubMed: 26015299]

[19]. Vaishya R, Agarwal AK, Tiwari M, Vaish A, Vijay V, Nigam Y, Journal of clinical orthopaedics and trauma, 9 (2017) S26–S33.

[20]. Zheng Z, Ran J, Chen W, Hu Y, Zhu T, Chen X, Yin Z, Heng BC, Feng G, Le H, Acta biomaterialia, 51 (2017) 317–329. [PubMed: 28093363]

[21]. Aibibu D, Hild M, Wöltje M, Cherif C, Journal of Materials Science: Materials in Medicine, 27 (2016) 63. [PubMed: 26800694]

[22]. Zhang W, Yang Y, Zhang K, Li Y, Fang G, Connective tissue research, 56 (2015) 25–34. [PubMed: 25333819]

[23]. Wu S, Wang Y, Streubel PN, Duan B, Acta biomaterialia, 62 (2017) 102–115. [PubMed: 28864251]

[24]. Wu S, Duan B, Liu P, Zhang C, Qin X, Butcher JT, ACS applied materials & interfaces, 8 (2016) 16950–16960. [PubMed: 27304080]

[25]. Hakimi O, Mouthuy P, Zargar N, Lostis E, Morrey M, Carr A, Acta biomaterialia, 26 (2015) 124–135. [PubMed: 26275911]

[26]. Han F, Zhao P, Lin C, Journal of Controlled Release, 259 (2017) e31.

[27]. Yang C, Deng G, Chen W, Ye X, Mo X, Colloids and Surfaces B: Biointerfaces, 122 (2014) 270–276. [PubMed: 25064476]

[28]. Bölgen N, Electrospun materials for bone and tendon/ligament tissue engineering, Electrospun Materials for Tissue Engineering and Biomedical Applications, Elsevier, 2017, pp. 233–260.

[29]. Jiang T, Carbone EJ, Lo KW-H, Laurencin CT, Progress in polymer Science, 46 (2015) 1–24.

[30]. Sun B, Long Y, Zhang H, Li M, Duvail J, Jiang X, Yin H, Progress in Polymer Science, 39 (2014) 862–890.

[31]. Cardwell RD, Dahlgren LA, Goldstein AS, Journal of tissue engineering and regenerative medicine, 8 (2014) 937–945. [PubMed: 23038413]

[32]. Shalumon K, Sheu C, Chen C-H, Chen S-H, Jose G, Kuo C-Y, Chen J-P, Acta biomaterialia, 72 (2018) 121–136. [PubMed: 29626695]

[33]. Bhaskar P, Bosworth LA, Wong R, O'brien MA, Kriel H, Smit E, McGrouther DA, Wong JK, Cartmell SH, Journal of Biomedical Materials Research Part A, 105 (2017) 389–397. [PubMed: 27649836]

[34]. Wu S, Peng H, Li X, Streubel PN, Liu Y, Duan B, Biofabrication, 9 (2017) 044106.

[35]. Rothrauff BB, Lauro BB, Yang G, Debski RE, Musahl V, Tuan RS, Tissue Engineering Part A, 23 (2017) 378–389. [PubMed: 28071988]

[36]. Wu J, Hong Y, Bioactive materials, 1 (2016) 56–64. [PubMed: 29744395]

[37]. Orr SB, Chainani A, Hippensteel KJ, Kishan A, Gilchrist C, Garrigues NW, Ruch DS, Guilak F, Little D, Acta biomaterialia, 24 (2015) 117–126. [PubMed: 26079676]

[38]. Alves A, Stewart AA, Dudhia J, Kasashima Y, Goodship AE, Smith RK, Veterinary Clinics: Equine Practice, 27 (2011) 315–333. [PubMed: 21872761]

[39]. Rubio-Azpeitia E, Sánchez P, Delgado D, Andia I, Orthopaedic Journal of Sports Medicine, 5 (2017) 2325967117690846.

[40]. Wu T, Liu Y, Wang B, Sun Y, Xu J, Yuk-wai LW, Xu L, Zhang J, Li G, Tissue Engineering Part A, 22 (2016) 1229–1240. [PubMed: 27609185]

[41]. Vuornos K, Björninen M, Talvitie E, Paakinaho K, Kellomäki M, Huhtala H, Miettinen S, Seppänen-Kaijansinkko R, Haimi S, Tissue Engineering Part A, 22 (2016) 513–523. [PubMed: 26919401]

[42]. Moshaverinia A, Xu X, Chen C, Ansari S, Zadeh HH, Snead ML, Shi S, Biomaterials, 35 (2014) 2642–2650. [PubMed: 24397989]

[43]. Zhang C, Wang X, Zhang E, Yang L, Yuan H, Tu W, Zhang H, Yin Z, Shen W, Chen X, Acta biomaterialia, 66 (2018) 141–156. [PubMed: 28963019]

[44]. Perikamana SKM, Lee J, Ahmad T, Kim EM, Byun H, Lee S, Shin H, Biomaterials, 165 (2018) 79–93. [PubMed: 29522987]

[45]. Suwalski A, Dabboue H, Delalande A, Bensamoun SF, Canon F, Midoux P, Saillant G, Klatzmann D, Salvetat J-P, Pichon C, Biomaterials, 31 (2010) 5237–5245. [PubMed: 20334910]

[46]. Zhao X, Jiang S, Liu S, Chen S, Lin ZYW, Pan G, He F, Li F, Fan C, Cui W, Biomaterials, 61 (2015) 61–74. [PubMed: 25996412]

[47]. Sun J, Mou C, Shi Q, Chen B, Hou X, Zhang W, Li X, Zhuang Y, Shi J, Chen Y, Biomaterials, 162 (2018) 22–33. [PubMed: 29428676]

[48]. Brady RD, Grills BL, Schuijers JA, Ward AR, Tonkin BA, Walsh NC, McDonald SJ, Journal of Orthopaedic Research, 32 (2014) 1277–1282. [PubMed: 25042765]

[49]. Tan WK, Purnamawati K, Pakkiri LS, Tan SH, Yang X, Chan MY, Drum CL, Expert opinion on biological therapy, (2018) 1–7.

[50]. Ti D, Hao H, Xia L, Tong C, Liu J, Dong L, Xu S, Zhao Y, Liu H, Fu X, Tissue Engineering Part A, 21 (2014) 541–549. [PubMed: 25204972]

[51]. Lee S-I, Yi J-K, Bae W-J, Lee S, Cha H-J, Kim E-C, PloS one, 11 (2016) e0146708. [PubMed: 26789270]

[52]. Pardon M-C, Expert opinion on biological therapy, 18 (2018) 165–169. [PubMed: 30063850]

[53]. Xu B, Yang M, Li Z, Zhang Y, Jiang Z, Guan S, Jiang D, Regulatory peptides, 184 (2013) 1–5. [PubMed: 23523891]

[54]. Santra M, Chopp M, Santra S, Nallani A, Vyas S, Zhang ZG, Morris DC, Journal of neurochemistry, 136 (2016) 118–132. [PubMed: 26466330]

[55]. Weinberger F, Nicol P, Starbatty J, Stubbendorff M, Becher PM, Schrepfer S, Eschenhagen T, Pharmacology research & perspectives, 6 (2018) e00407. [PubMed: 29864245]

[56]. Wu S, Duan B, Qin X, Butcher JT, Acta biomaterialia, 51 (2017) 89–100. [PubMed: 28110071]

[57]. Wu Y, Han Y, Wong YS, Fuh JYH, Journal of tissue engineering and regenerative medicine, (2018).

[58]. Liu Y, Ramanath H, Wang D-A, Trends in biotechnology, 26 (2008) 201–209. [PubMed: 18295915]

[59]. Yang G, Lin H, Rothrauff BB, Yu S, Tuan RS, Acta biomaterialia, 35 (2016) 68–76. [PubMed: 26945631]

[60]. Fallahi A, Khademhosseini A, Tamayol A, Trends in biotechnology, 34 (2016) 683–685. [PubMed: 27499277]

[61]. Santos ML, Rodrigues MT, Domingues RM, Reis RL, Gomes ME, Biomaterials as tendon and ligament substitutes: Current developments, Regenerative Strategies for the Treatment of Knee Joint Disabilities, Springer, 2017, pp. 349–371.

[62]. Kendal A, Snelling S, Dakin S, Stace E, Mouthuy P, Carr A, Eur. Cell Mater, 33 (2017) 169–182. [PubMed: 28266691]

[63]. Xue J, Xie J, Liu W, Xia Y, Accounts of chemical research, 50 (2017) 1976–1987. [PubMed: 28777535]

[64]. Lomas A, English A, Biggs M, Pandit A, Zeugolis DI, Engineering Anisotropic 2D and 3D Structures for Tendon Repair and Regeneration, Tendon Regeneration, Elsevier, 2015, pp. 225–242.

[65]. Lee NM, Erisken C, Iskratsch T, Sheetz M, Levine WN, Lu HH, Biomaterials, 112 (2017) 303–312. [PubMed: 27770633]

[66]. Kösters A, Wiesinger H, Bojsen-Møller J, Müller E, Seynnes OR, Clinical Biomechanics, 29 (2014) 323–329. [PubMed: 24405566]

[67]. Geremia JM, Bobbert MF, Nova MC, Ott RD, de Aguiar Lemos F, de Oliveira Lupion R, Frasson VB, Vaz MA, Clinical Biomechanics, 30 (2015) 485–492. [PubMed: 25828432]

[68]. Sánchez M, Anitua E, Azofra J, Andía I, Padilla S, Mujika I, The American journal of sports medicine, 35 (2007) 245–251. [PubMed: 17099241]

[69]. Chan B, Leong K, European spine journal, 17 (2008) 467–479. [PubMed: 19005702]

[70]. Di Marcantonio L, Russo V, Wyrwa R, Walter T, Schnabelrauch M, Barboni B, (2016).

[71]. Lipner J, Liu W, Liu Y, Boyle J, Genin G, Xia Y, Thomopoulos S, Journal of the mechanical behavior of biomedical materials, 40 (2014) 59–68. [PubMed: 25194525]

[72]. Lohan A, Kohl B, Meier C, Schulze-Tanzil G, International journal of molecular sciences, 19 (2018) 2059.

[73]. Song B, Li W, Chen Z, Fu G, Li C, Liu W, Li Y, Qin L, Ding Y, Journal of Orthopaedic Translation, 8 (2017) 32–39. [PubMed: 30035092]

[74]. Ratner BD, Hoffman AS, Schoen FJ, Lemons JE, Biomaterials science: an introduction to materials in medicine, Elsevier, 2004.

[75]. Jenkins TL, Meehan S, Pourdeyhimi B, Little D, Tissue Engineering Part A, 23 (2017) 958–967. [PubMed: 28816097]

[76]. Araque-Monrós MC, Vidaurre A, Gil-Santos L, Bernabé SG, Monleón-Pradas M, Más-Estellés J, Polymer degradation and stability, 98 (2013) 1563–1570.

[77]. Teo AJ, Mishra A, Park I, Kim Y-J, Park W-T, Yoon Y-J, ACS Biomaterials Science & Engineering, 2 (2016) 454–472.

[78]. Maghdouri-White Y, Petrova S, Sori N, Polk S, Wriggers H, Ogle R, Ogle R, Francis M, Biomedical Physics & Engineering Express, 4 (2018) 025013.

[79]. Domingues RM, Chiera S, Gershovich P, Motta A, Reis RL, Gomes ME, Frontiers in Bioengineering and Biotechnology, 4 (2016).

[80]. Via AG, McCarthy MB, de Girolamo L, Ragni E, Oliva F, Maffulli N, Sports medicine and arthroscopy review, 26 (2018) 64–69. [PubMed: 29722765]

[81]. Eagan MJ, Zuk PA, Zhao KW, Bluth BE, Brinkmann EJ, Wu BM, McAllister DR, Journal of tissue engineering and regenerative medicine, 6 (2012) 702–709. [PubMed: 21953999]

[82]. Gonçalves AI, Rodrigues MT, Lee S-J, Atala A, Yoo JJ, Reis RL, Gomes ME, PloS one, 8 (2013) e83734. [PubMed: 24386267]

[83]. Ziaei M, Greene C, Green CR, Advanced drug delivery reviews, 126 (2018) 162–176. [PubMed: 29355667]

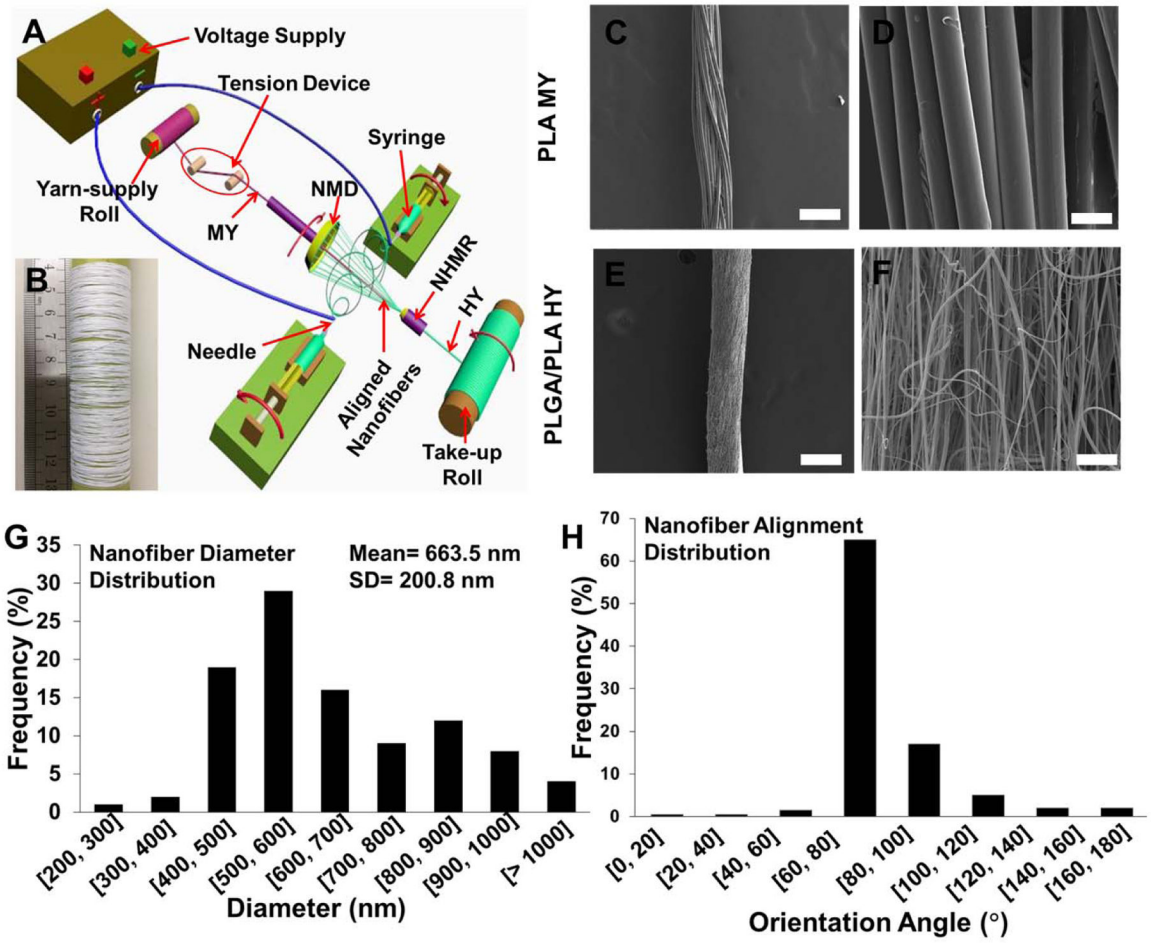

Fig. 1.

Fabrication of PLGA/PLA nanofiber/microfiber HY. (A) Schematic illustration of the modified electrospinning system for coating electrospun PLGA nanofibers on the surface of PLA MY to generate PLGA/PLA HY. (B) Photograph of a PLGA/PLA HY package with fabrication and electrospinning for 4 hours. (C, D) SEM images of the original PLA MY; (E, F) SEM images of the obtained PLGA/PLA HY. Scale bars: 200 μm for (C) and (E); 20 μm for (D) and (F). (G) Fiber diameter distribution of PLGA nanofibers on the surface of PLGA/PLA HY. (H) Orientation angular distribution measurement of the PLGA nanofibers on the surface of PLGA/PLA HY.

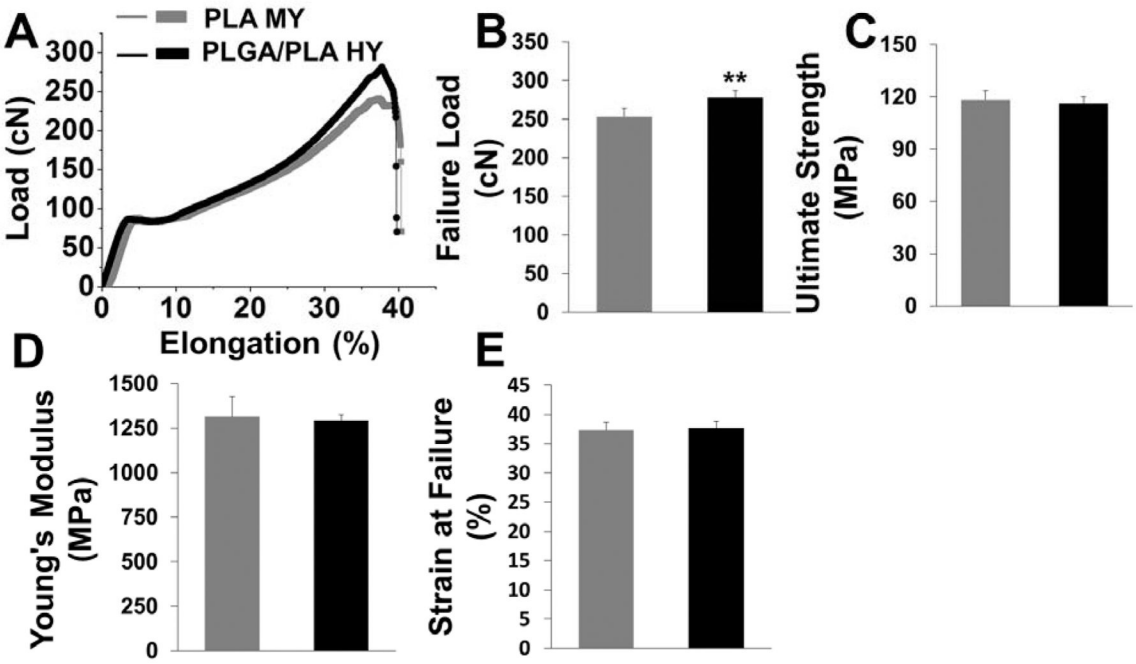

Fig. 2.

Characterization of tensile properties of PLA MY and PLGA/PLA HY. (A) Representative stress-strain curves. (B) Failure load (C) Ultimate tensile strength. (D) Young's modulus. (E) Strain at failure. (n=20; ** p<0.01.)

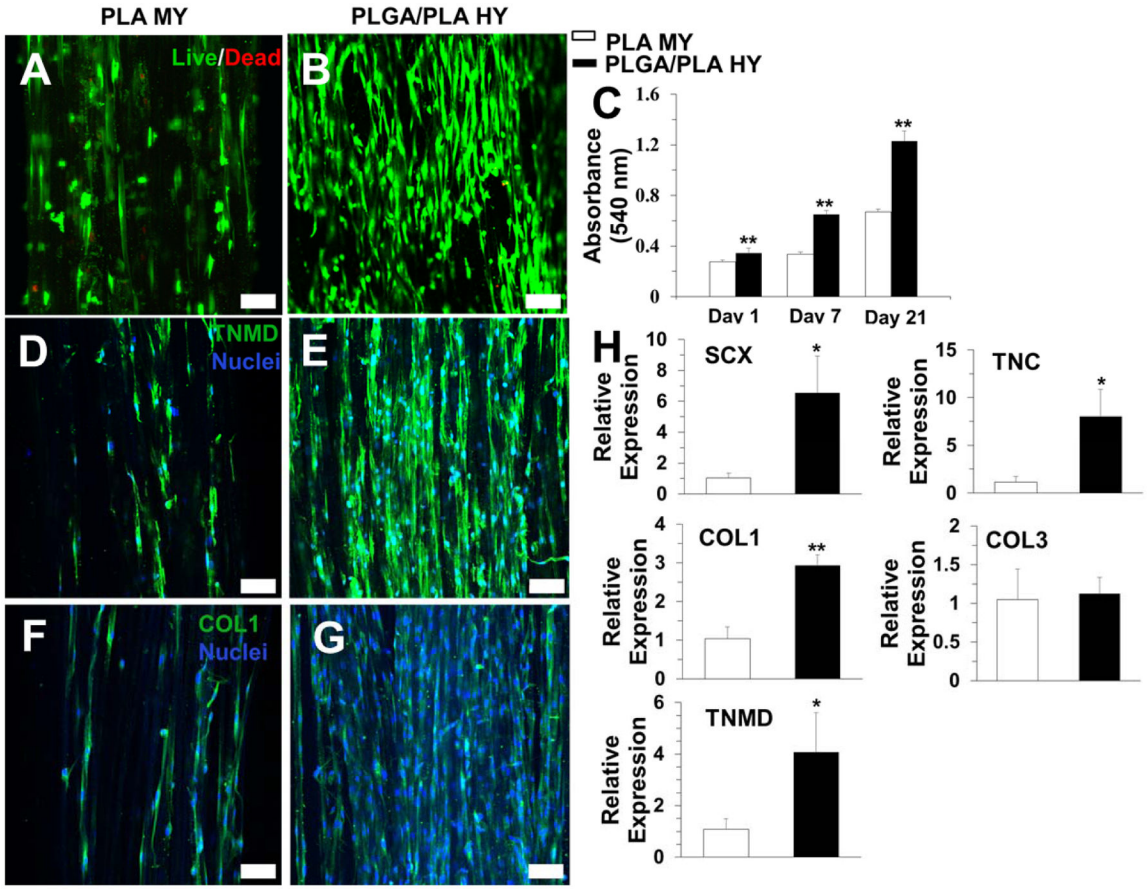

Fig. 3.

The coating of PLGA nanofibers on the surface of PLGA/PLA HY promoted HADMSC alignment, proliferation, and tenogenic differentiation. (A, B) Representative fluorescent images of living cells (green) and dead cells (red) of HADMSC seeded on PLA MY bundles and PLGA/PLA HY bundles conditioned in TM for 21 days. Scale bar: 100 μm. (C) Cell proliferation quantification by MTT assay at day1, 7, and 21 for HADMSC cultured on the two different yarn bundles in TM (n=5; $^{**}p<0.01$). (D, E) IF staining for TNMD (green), and nuclei (blue) of HADMSC after 21-day tenogenic differentiation. Scale bar: 100 μm. (F, G) IF staining for COL1 (green), and nuclei (blue) of HADMSC after 21-day tenogenic differantiation. Scale bar: 100 μm. (H) qPCR analysis of SCX, TNC, COL1A1, COL3A1, and TNMD gene expression on HADMSC-seeded PLA MY and PLGA/PLA HY bundles. Relative gene expression is presented as normalized to 18S and expressed relative to HADMSC-seeded PLA MY bundles (n=3; $^{*}p<0.05$, $^{**}p<0.01$)

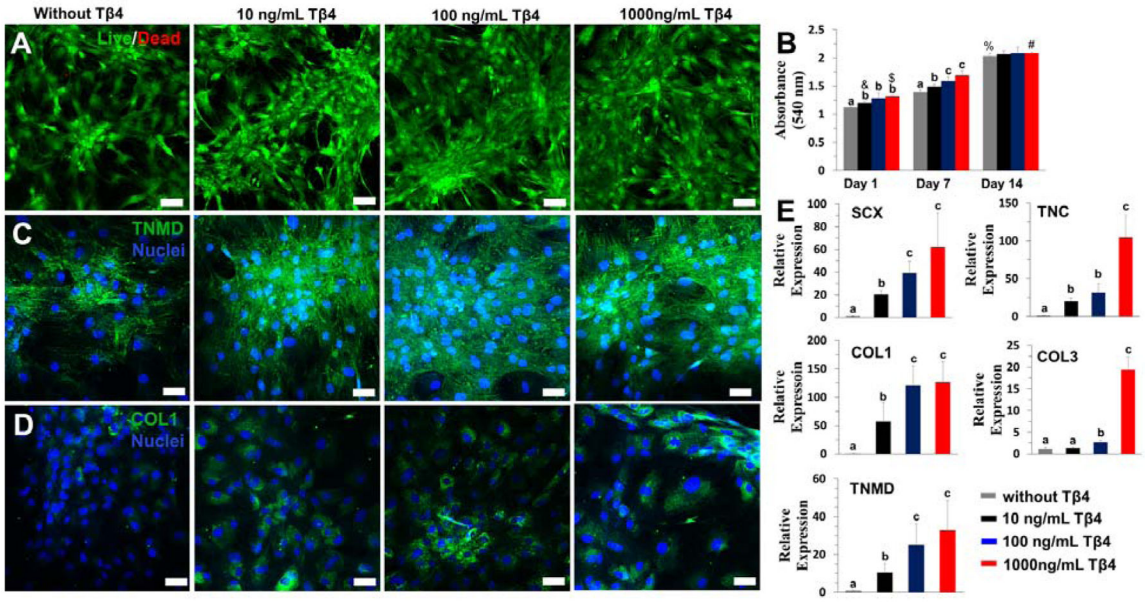

Fig. 4.

The dose and time-dependent effects of Tβ4 on the proliferation rate, and tenogenic differentiation of HADMSC in 2D culture. (A) Live/Dead images for HADMSC treated with different doses of Tβ4 for 14 days. Scale bars: 100 μm. (B) MTT results of HADMSC cultured by different concentrations of Tβ4 at day1, 7 and 14 (n=5; bars that do not share letters are significantly different from each other (p<0.05), there is a statistical difference between the groups with "&" and "$", also between "%" and "#" (p<0.05)). (C, D) IF staining for tendon-associated proteins (TNMD, and COL1) for HADMSC treated with different doses of Tβ4 for 14 days. Scale bars: 100 μm. (E) qPCR analysis of SCX, TNC, COL1A1, COL3A1, and TNMD gene expression of HADMSC treated with different doses of Tβ4 for 14-day culture. Relative gene expression is presented as normalized to 18S expressed relative to HADMSC none-treated with Tβ4. (n=3; bars that do not share letters are significantly different from each other (p<0.05)).

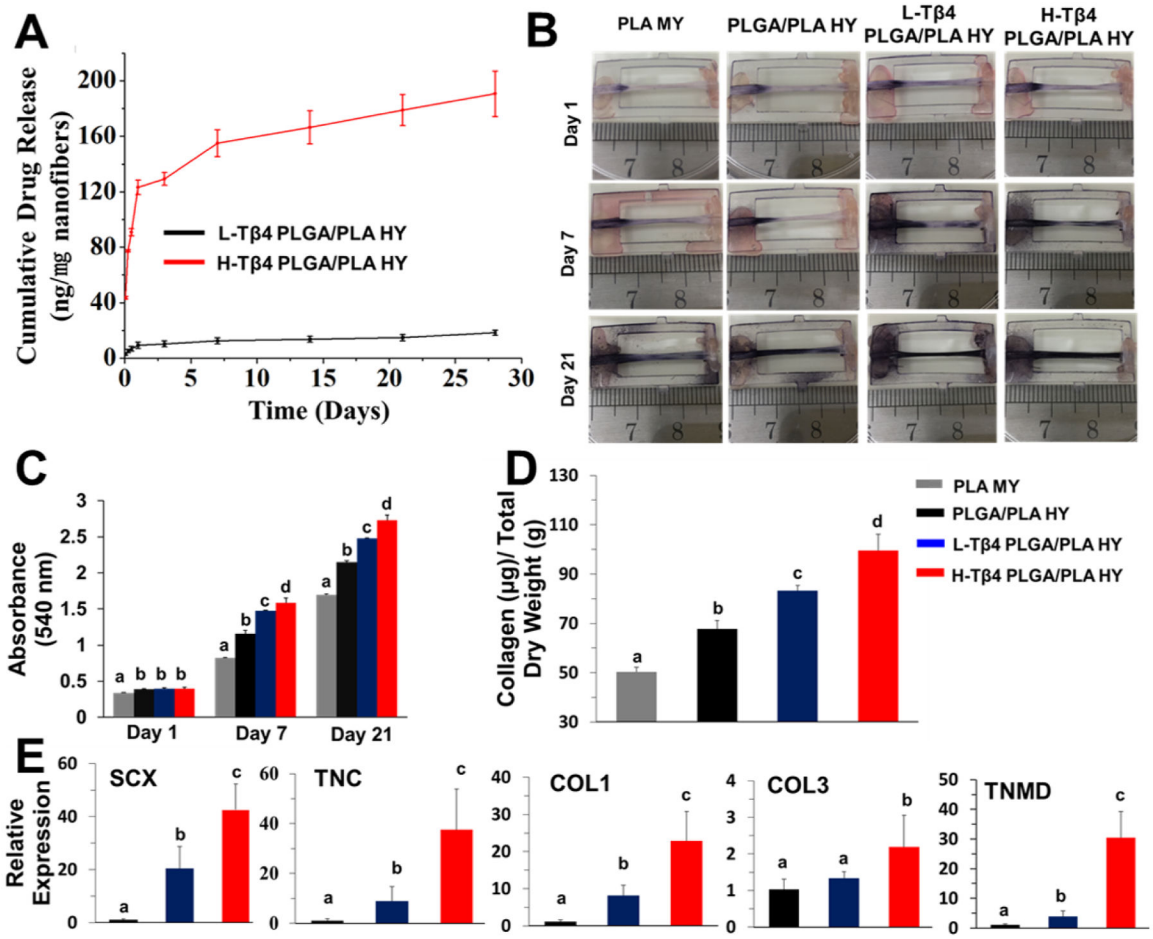

Fig. 5.

The incorporation of Tβ4 enhanced cell proliferation, directional alignment and migration, collagen secretion, and tenogenic differentiation. (A) Cumulative release of Tβ4 from PLGA/PLA HY with different dosages of Tβ4 after incubation in PBS at 37 °C. (B) The dose and time-dependent effects of Tβ4 on the migration of HADMSC seeded on PLA MY and PLGA/PLA HY bundles. (C) The effects of Tβ4 on the proliferation rate of HADMSC seeded on PLA MY and PLGA/PLA HY bundles with and without Tβ4. (n=5; bars that do not share letters are significantly different from each other (p<0.05), and comparative analysis between the four different groups was only conducted for the same time point). (D) Total collagen content of HADMSC seeded on four different yarn bundles for 21-day culture. (n=5; bars that do not share letters are significantly different from each other (p<0.05)). (E) qPCR analysis of tendon-related genes (SCX, TNC, COL1A1, COL3A1, and TNMD) of HADMSC seeded on three PLGA/PLA HY bundles with and without Tβ4 for 21 days. Relative gene expression is presented as normalized to 18S and expressed relative to HADMSC seeded on PLGA/PLA HY without Tβ4 (n=3; bars that do not share letters are significantly different from each other (p<0.05)).